Post-print of the article:
L. Gurreri, M. La Cerva, J. Moreno, B. Goossens, A. Trunz, A. Tamburini, *Coupling of electromembrane processes with reverse osmosis for seawater desalination: Pilot plant demonstration and testing,* Desalination (2022) 526, 115541. https://doi.org/10.1016/j.desal.2021.115541

Coupling of electromembrane processes with reverse osmosis for seawater desalination: Pilot plant demonstration and testing

Luigi Gurreri[a*], Mariagiorgia La Cerva[a], Jordi Moreno[b], Berry Goossens[c], Andrea Trunz[d*] Alessandro Tamburini[a]

[a] *Department of Engineering, University of Palermo, Viale delle Scienze ed. 6, 90128 Palermo, Italy*

[b] *REDstack B.V., Graaf Adolfstraat 35G, 8606 BT Sneek, The Netherlands*

[c] *FUJIFILM Manufacturing Europe B.V., Oudenstaart 1, 5000 LJ Tilburg, the Netherlands*

[d] *Trunz Water Systems AG, Technologie Center, Ahornstrasse 1, CH-9323 Steinach, Switzerland*

*corresponding authors – email: luigi.gurreri@unipa.it, a.trunz@trunz.ch

ABSTRACT

Reverse osmosis (RO) is the most widespread technology to produce drinking water from seawater (SW). However, the integration of different membrane processes offers interesting alternatives. In this work, electromembrane processes were integrated with RO to desalinate real seawater in a pilot plant with 25 m^3/day capacity. Electrodialysis (ED, either two-stage or single stage), shortcut reverse electrodialysis (scRED) and assisted reverse electrodialysis (ARED) pre-desalinated seawater before RO with the ED-ED-RO, ED-RO, and scRED-ARED-RO process schemes. Treated wastewater was used as salt sink in the scRED-ARED tests. The performance of the pilot plant can be summarized as follows: water recovery of ~27-51%, productivity of ~7-14 L/(m^2 h) in the electromembrane processes and of ~19-31 L/(m^2 h) in the RO process, energy consumption of 3.5-8.4 kWh/m^3. The ED-RO configuration yielded the maximum productivity in the electromembrane step, while the scRED-ARED-RO integration reached the minimum energy consumption. Overall, the energy performance of the pilot plant (especially in the ED-RO and scRED-ARED-RO schemes) was comparable to that of a standalone SWRO system. The field tests demonstrated that the coupling of electromembrane processes with RO is feasible and suggest the possibility to develop alternative and competitive industrial pants for seawater desalination.

Keywords: ion-exchange membrane; field test; potable water; hybrid membrane process; impaired water.

1 Introduction

The increasing global water demand requires challenging solutions for a satisfactory water supply. Due to the abundance of saltwater, desalination will play a crucial role. Today the worldwide capacity of desalination plants is ~100 million m^3/day of freshwater, ~60% of which is obtained by using seawater (SW), and ~70% via the reverse osmosis (RO) technology [1,2]. Typical water fluxes of RO modules, which affect the capital cost, are in the range 10-40 L/(m^2 h) [3]. The operating costs are basically due to the energy consumed to pressurize the feedwater. The theoretical minimum energy (thermodynamic limit) consumed to produce freshwater from seawater with 50% water recovery is ~1 kWh/m^3 [4,5]. However, the overpressure required by RO to generate reasonable water fluxes and the steps of intake, pre- and post-treatment, and brine disposal significantly increase the energy consumption. On the other hand, part of the pressure energy can be recovered by pressure exchangers. The specific energy consumption (SEC) of SWRO desalination plants has been reduced significantly in the last decades [4,5], being now in the range 2.5–7 kWh/m^3 [5–10].

Electrodialysis (ED) [11] is an emerging technology [12] that holds ~2-3% of the global desalination capacity [1,2,6]. ED desalination plants use brackish water to produce potable water, as ED can compete with RO for low-salinity feeds. Predictions of a process model showed that ED outperforms RO in terms of energy consumption to desalinate feedwater at a concentration lower than 3 g/L [13]. On the other hand, the high cost of the IEMs (in the order of 10-100 €/m^2 [14,15], against ~10 €/m^2 of osmotic membrane for RO [16]) still limits a widespread use of ED. However, another study found that ED is economically convenient compared to RO for a feedwater salinity below ~8 g/L [17].

ED is also versatile for various applications [18,19]. However, it is techno-economically uncompetitive with SWRO yet to produce freshwater by desalinating concentrated solutions like seawater [20–27]. The low concentration of the dilute product (e.g., ~0.5 g/L) and the large concentration gradient between the two compartments (up to ~60 g/L) cause low migrative fluxes and high back diffusive fluxes, respectively, in a portion of the stack ending with the outlet, resulting in

low net fluxes. This implies that the SWED process has difficulties in reaching the concentration target for drinking water. Multi-staging is an effective strategy to produce potable water by the application of current densities approaching the limiting one of each stage. Moreover, increasing the membrane area reduces the SEC [12]. A process model simulated a two-stage SWED process with cross-flow stacks equipped with profiled membranes, predicting low (or high) values of SEC along with low (or high) values of productivity in the range of ~2.3-5.7 kWh/m^3 and ~2.6-11.2 L/(m^2 h), respectively [23]. A three-stage ED system used in experiments with natural seawater (~27 g/L) produced a diluate at 1.9 g/L with an SEC of ~3 kWh/m^3 and a productivity, here estimated by neglecting water transport, of ~6 L/(m^2 h) [24]. These examples show that multi-stage SWED processes can produce potable water, but only one of the two performance metrics (SEC or productivity) at a time has values comparable with those typical of RO.

The opposite process of ED is reverse electrodialysis (RED), which converts the mixing energy of two solutions at different salt concentration into electrical energy. The RED process has been widely studied in the last decade [15,28–31] and pilot installations have brought the technology maturity to the prototype level [32–36]. However, industrial applications do not exist yet due to the low power density (in the order of 1 W/m^2 for seawater-river water, one order of magnitude more in the case of acidic and alkaline solutions in stacks with bipolar membranes [37]) and high membrane cost.

RED can be a method of simultaneous seawater pre-desalination and energy recovery by using a salt sink, such as impaired water [38]. A RED stack operated with null external resistance works under short-circuit conditions (scRED), producing the maximum current along with zero voltage, i.e., without energy recovery nor consumption (apart from the pumping energy). Therefore, it yields the maximum desalination degree with a spontaneous process. RED can also be conducted under "assisted" conditions. Assisted reverse electrodialysis (ARED) has hybrid features between ED and RED, as it uses electricity from a power supply (like ED) in addition to that generated by a salinity gradient (like RED) to drive electromigration from the high-salinity compartment to the low-salinity

compartment (like RED). By applying a voltage drop of opposite sign compared to RED, the electric current of ARED is higher than the short-circuit value. Therefore, ARED consumes energy by desalting the high-salinity solution either more than RED or with less membrane area than RED.

Hybridization of membrane technologies has been proposed as a strategy for the development of energy efficient desalination processes [10,12,39]. Coupling RO with the abovementioned electromembrane (EM) processes (ED, RED or ARED) offers several solutions. Many studies have focused on minimum liquid discharge concepts where the RO reject brine valorisation is performed via (i) ED and crystallization to recover water and salt, or (ii) ED with bipolar membranes to produce acid and base, or (iii) RED to recover energy [12,19,40].

Other hybrid schemes can be devised with EM processes used as a pre-treatment step before RO to desalinate seawater. The SWED-RO system (Figure 1a) may enhance the energy efficiency compared to the standalone processes. The partial desalination in the ED stage, which works under milder conditions (i.e., with higher limiting current density, lower back-diffusion and higher current efficiency) than those of the SWED process producing potable water, may be cost-effective [41,42] by achieving high productivity and efficiency [41]. Moreover, the ED versatility in terms of desalination degree and water recovery makes it potentially suitable as pre-treatment before RO. This would then receive a brackish water with lower osmotic pressure that would require lower operating pressures or lower membrane area, and could achieve high water recoveries. By performing batch ED experiments with artificial seawater, Galama *et al.* [43] used literature data on BWRO and estimated an SEC of the SWED-RO desalination of ~3 kWh/m^3, against an SEC of the standalone SWED higher by 6%. Post *et al.* [44] performed a cost analysis of desalination processes. In a perspective scenario with high-performance and low-cost IEMs (perfect permselectivity, no water transport, 5 €/m^2), the SWED-RO configuration with 80% pre-desalination was effective in reducing the water cost. The authors of the present paper from the University of Palermo presented a cost analysis based on the predictions of process models [38]. Some conditions simulated for the hybrid SWED-RO process

(lower voltage and higher number of cell pairs) exhibited a reduction of SEC compared to the standalone SWRO, but it was small. The SWED-RO desalination cost was higher in all cases, showing that the conditions simulated were not optimal. An optimization study of hybrid systems (ED-RO, NF-RO, NF-ED-RO, and FO-ED-RO) for seawater desalination was performed together with a carbon footprint evaluation and a cost analysis [45]. The objective function of minimum SEC was used, and the ED-RO system achieved the lowest value (1.3 kWh/m^3) along with a reduction of CO_2 emissions. However, searching for the minimum SEC resulted in low water recoveries (< 30%) and large IEMs area, increasing the water cost.

The ED-RO hybridization was also studied for other applications, including brackish water desalination [46,47], groundwater treatment [48], and near-zero liquid discharge approaches to treat basal aquifer water [49] or desulfurization wastewater [50], showing promising results.

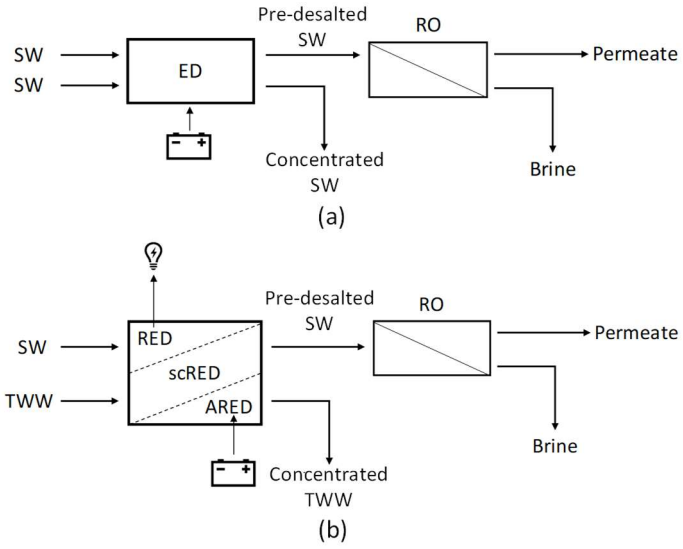

Figure 1. Schematics of hybrid systems for seawater (SW) desalination with reverse osmosis (RO) coupled with electromembrane pre-treatments: (a) electrodialysis (ED); (b) reverse electrodialysis (RED), short-circuit reverse electrodialysis (scRED) or assisted reverse electrodialysis (ARED) using treated wastewater (TWW as "salt sink". Adapted from [38].

In the RED-RO and ARED-RO couplings for seawater desalination, the EM process is performed by exploiting a sink of salt represented by impaired water that cannot be used directly to produce

freshwater, e.g., treated wastewater (Figure 1b). The energy efficiency of the desalination process is enhanced compared to the ED-RO system thanks to a completely (RED or scRED) or partially (ARED) spontaneous pre-desalination. The RED process also supplies electrical energy to an external load. RED experiments showed that the salt concentrations in the low-salinity solution that maximize the power density (0.39 W/m^2) were between 0.01 and 0.02 M [51]. This range, which was confirmed by several studies [52,53], corresponds to typical concentrations of treated wastewater (TWW) from biological processes. With real pre-treated solutions, a maximum gross power density of 1.43 W/m^2 was obtained [54]. Therefore, RED using the SW-TWW solutions could be adopted as RO pre-treatment to reduce the SEC. The other option is SWRO-RED, in which RED uses the RO brine-TWW solutions, thus increasing the energy production [51]. However, Li *et al*. [55] showed a lower SEC for the RED-RO configuration (~0.5 kWh/m^3) compared to the RO-RED scheme (~1 kWh/m^3). With lab-scale experiments, Vanoppen *et al*. [56,57] found that, compared to RED, ARED boosts the desalination degree with low energy consumption due to a significant reduction of stack resistance (higher average concentration of the low-salinity stream) at high current densities. The reduction of resistance and its effects may vanish in large-scale stacks. However, the ARED option can improve the process economics. At high water recoveries (> 40%) the estimated SEC of the ARED-RO process was lower than that of the standalone RO, but larger than that of RED-RO [56]. Nevertheless, the lower membrane requirement of ARED pre-treatments and their resulting lower investment costs reduced the water cost of ARED-RO hybrid systems compared to RED-RO. A water cost reduction compared to the standalone SWRO was found when the IEMs cost was lower than 10 €/m^2 [56]. Our simulations and economic analysis showed that both RED-RO and ARED-RO may achieve cost savings compared to the standalone SWRO even with a cost for the EM stack of 40 €/m^2 [38].

The present literature review shows that hybrid schemes coupling EM processes with RO (i.e., ED-RO, RED-RO, and ARED-RO systems) offer new opportunities to reduce the energy consumption and even the specific cost of desalination. However, a poor effort has been devoted to the development

of these systems for seawater desalination, and more studies are needed at pilot-scale to enhance the technological readiness level of emerging processes [12,40]. In this work, we present the first experimental proof-of-concept of electromembrane processes-RO coupling for seawater desalination by the development, construction, and testing of a pilot plant with a capacity of 25 m^3/day working in a real environment. The plant was tested under various operating conditions during a period of about one year, and the collected data are presented and discussed in this paper.

2 Experimental

The pilot installation targeted an integrated ED/RED-RO system with a capacity of 25 m^3/day of desalinated water. The system was designed to facilitate flexible testing of one stage or two-stage ED/RED/ARED pre-desalination using real seawater and, in the case of RED or ARED, treated wastewater.

The test location was at the facilities of the municipal wastewater treatment plant located in Burriana (province of Valencia), Spain, which is placed close to the sea. The plant belongs to FACSA, a Spanish private company specialized in water cycle management. The desalination pilot plant was constructed by Trunz in a containerised system (Figure 2). The programming of the PLC was done in order to perform controlled long-time testing, including a remote monitoring. During the experiments, all parameters (including flow rate, pH, conductivity, electric current, voltage drop and pressure) were measured by the installed instruments and saved by a data acquisition system for later elaboration.

Figure 2. Picture of the integrated EM process-RO pilot plant (left) installed in a container (right) at the FACSA WWTP in Burriana, Spain.

The technical concept of the pilot plant consisted out of three main systems:

1. The pre-treatment system of the seawater and wastewater, preventing fouling and scaling problems in the membranes of the EM and RO systems;
2. The EM system consisting of 2 stacks, which partially desalinated the seawater;
3. The RO system, finalising the desalination process to produce drinking water.

2.1 Pre-treatment system

The main physico-chemical characteristics of the two feeds (i.e., seawater and secondary treated wastewater) are reported in Table 1 and Table 2, respectively.

Table 1. Physico-chemical properties of seawater samples.

Parameter	Units	Value
Sodium	(mg/L)	12122.5
Magnesium	(mg/L)	1383.5
Calcium	(mg/L)	619.3
Potassium	(mg/L)	441.3
Chloride	(mg/L)	21010.2
Sulfate	(mg/L)	2936.0
Bromide	(mg/L)	58.8
Fluoride	(mg/L)	0.8

TOC	(mg/L)	3.6
TC	(mg/L)	30.2
TDS	(mg/L)	38572.4
Conductivity	(mS/cm)	52.1
pH		7.7
Alkalinity (as CaCO3)	(mg/L)	126.3

177

178 Table 2. Physico-chemical properties of secondary treated wastewater samples.

Parameter	Units	Value
TOC	(mg/L)	9
TDS	(mg/L)	1484
Conductivity	(mS/cm)	2.2
pH		7.9
Alkalinity (as CaCO3)	(mg/L)	150
Turbidity	(NTU)	4
Suspended solids (glass fiber)	(mg/L)	5
BOD5	(mg/L)	8
COD	(mg/L)	19

179 The pre-treatment system was designed to guarantee an advanced protection of the EM-RO units and
180 of the pumps. The goal of the pre-treatment of the feedwater (seawater or wastewater) was to prevent
181 fouling and clogging in the integrated desalination pilot plant by removing suspended solids, organic
182 matter, and microorganisms.

183 The pre-treatment system had one line dedicated to only seawater and two lines in parallel for
184 wastewater.

185 As a first pre-treatment step, a sand filtration was used. The advantage of a sand filter is its back-
186 flushing possibility. A cartridge filter (100 µm MF), which is cheap and easily handling, was then
187 chosen as the second step.

188 The heart of the pre-treatment was an ultrafiltration (UF) module (Inge VK-0069 Dizzer XL 1.5 MB
189 40 W, Lenntech) that removes organic contamination down to a size of 0,02 µm. The UF pre-
190 treatment was controlled with a manual back and forward flushing and required very little
191 maintenance, ensuring safe operation of the entire system.

In addition, the two lines for wastewater included active carbon filters (Big Blue, 20" cartridge filter, Pentair) as a further step after ultrafiltration.

2.2 Electromembrane system

Preliminary estimates resulted in the idea to use a 2-stage EM system at low flow velocity to perform the pre-desalination of seawater before RO. This system should be characterized by low values of energy consumption. A 1-stage ED system, which requires less membrane area, was also considered, as it is intrinsically characterized by higher values of productivity.

The stacks (REDstack B.V., the Netherlands, Figure 3) were with cross-flow layout of the fluid streams and each of them contained 288 cell pairs of Fujifilm Type 10 membranes (FUJIFILM Manufacturing Europe B.V., the Netherlands) with active area of 0.44×0.44 m^2. The main properties of the membranes are reported in Table 3. Polymeric spacers with woven net and of 260 μm thickness (Deukum GmbH, Germany) were used to separate the membranes and create the channels.

Pt-coated Ti-mesh electrodes (Magneto Special Anodes B.V., The Netherlands) were used. The electrode rinse solution (ERS) was an aqueous solution with 0.5M Na_2SO_4. Either FUJIFILM Type 10 or Fumasep® F-10100 (Fumatech GmbH, Germany) CEMs were used as end-membranes confining the electrode compartments (for more details, see the Appendix).

The electrode compartments of the ED stacks were connected to a DC power supply (SM 500-CP-90, Delta Elektronika, The Netherlands). The solutions were fed into the stacks by centrifugal pumps (MDR 85 P3-1V, Johnson Pump).

The pilot installation was used either for Electrodialysis (ED) of seawater or Assisted Reverse Electrodialysis (ARED) of the couple seawater / wastewater. The feed water from the pre-treatment was transferred to either the diluate or the concentrate tank. From these tanks the feed water was then pumped into the ED stacks.

Problems of biofouling and calcium-carbonate scaling in the stacks may be expected. The pre-treatment step based on ultrafiltration was combined with acid dosing in the ED stacks. In addition, the electrodialysis reversal operation (switch every 30 minutes) was performed. A possibility to perform chemical cleaning-in-place (CIP) was also included.

The combined action of the advanced pre-treatment system, of the polarity reversal, and of the chemical dosage succeeded in the purpose of protecting the pilot plant, allowing a long operation without a performance drop. For industrial applications, concerns may arise on the economic viability of the applied methods. Therefore, purposely devoted studies should address this specific aspect.

The pilot installation was equipped with the necessary tools to measure flow, pressure, temperature, conductivity, and pH in all streams.

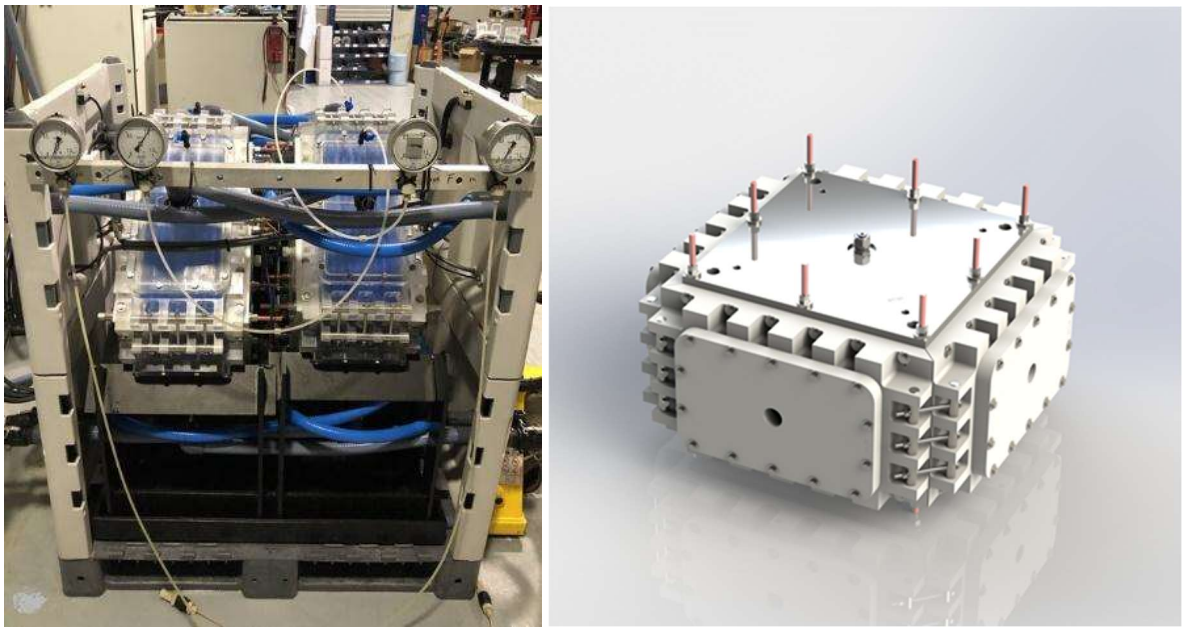

Figure 3. Picture of the 2-stack EM pilot (left) and 3D drawing of one stack designed by REDstack.

Table 3. Properties of the Fujifilm Type 10 ion-exchange membranes used in this study.

	Thickness (dry) [µm]	**Areal resistance[a] [Ω cm^2]**	**Permselectivity[b] [%]**	**IEC [meq/g]**	**Water permeability [ml/(m^2 h bar]**	**Burst strenght [kg/cm^2]**
AEM	125	1.7	95	1.8	6.5	2.8

CEM	135	2.0	99	1.5	6.5	2.8

[a] Measured in 2 M NaCl solution.

[b] Evaluated from measurements of membrane potential with 0.05 M and 0.5 M KCl solutions.

2.3 RO system

The RO setup was designed for processing pre-desalinated water from the ED system. The technical considerations for this design were a maximum value of TDS in the feed of ~20 g/l, Silt Density Index (SDI) < 2.5 (ensured by the pre-treatment train), permeate flowrate of about 25 m^3/day, TDS in the permeate < 0.5 g/L, and water recovery up to ~70%.

FilmTec^{TM} SW30-4040 elements with 7.4 m^2 of active area each (polyamide thin-film composite membrane, DuPont Water Solutions) were selected. The main test conditions and the relevant results indicated by the manufacturer in the datasheet are: 32,000 ppm NaCl feed, applied pressure of 55 bar, 7.4 m^3/day permeate flowrate with 8% water recovery. One pressure vessel with six RO elements was selected and constructed for the pilot plant. An acid dosing system was implemented for the RO modules due to the possible presence of carbonate species and a high pH (close to 8) in the feedwaters.

After chemical dosage, a high-pressure pump (180B3046 APP 2.5, Danfoss) fed the RO pressure vessel.

2.4 Experimental plan

The tested configurations of the pilot plant were ED-ED-RO, ED-RO, and scRED-ARED-RO, as schematically illustrated in Figure 4. The double-stage of ED was adopted to boost the pre-desalination rate. An opposite strategy was adopted with the single-stage ED, which has a halved IEM area (and thus higher productivity) and can achieve a lower pre-desalination rate, due to the limiting current. The scRED-ARED configuration is somehow an intermediate case, because it had the same membrane area as the ED-ED configuration, but it was characterized by a lower total current value, which was similar to that of the single-stage ED (Section 3.1).

All field tests were conducted with the simple one-pass operation. Either one-stage or two-stage EM pre-desalination operation was tested. In the ED-RO tests, pre-treated seawater was fed into both the diluate and concentrate compartments of the first ED stack. In the ARED-RO tests, pre-treated seawater and wastewater were fed into the concentrate and diluate compartments, respectively, of the first stack. In the cases of two-stage EM pre-desalination, the second stack was fed by the outlet solutions coming from the first one.

The pre-desalted seawater produced by the EM processes (either ED or ARED) was collected in a buffer tank and pumped into the RO pressure vessel.

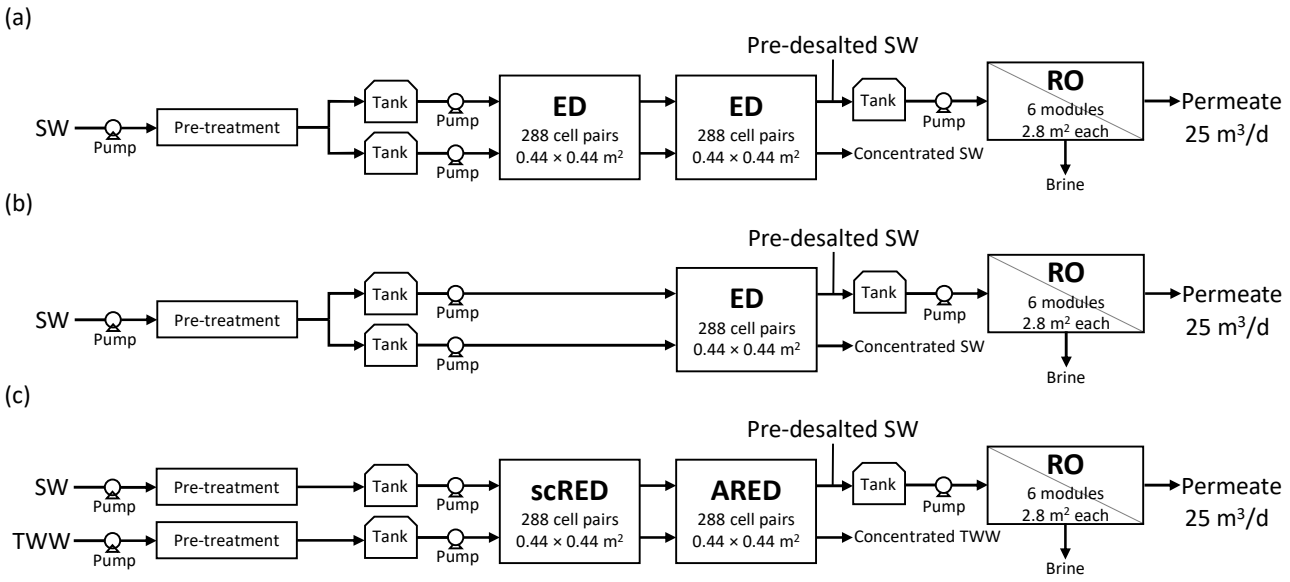

Figure 4. Schematic diagrams of the tested pilot plant configurations: (a) ED-ED-RO, (b) ED-RO, and (c) scRED-ARED-RO.

Several tests were performed by letting the set points of the EM pre-desalination vary, as reported in Table 4. The test cases 1-7, 8, and 9-10 are for the ED-ED-RO, ED-RO (single stage ED before RO), and scRED-ARED-RO configuration, respectively. The outlet flow rates from the two compartments were chosen to have a water recovery in the EM pre-desalination around 63%. The pressure applied in the RO stage was adjusted to produce a nominal flow rate of permeate of 25 m^3/day (±30%), corresponding to a total water recovery around 40%. The EM pre-desalination rate ranged from 35% to 51%. Clearly, RO completed the desalination process producing drinking water.

The EM processes were conducted with asymmetric flow rates. In particular, the flow rate of the pre-desalinated SW was higher than the flow rate of pre-concentrated solution (SW or TWW), aiming at increasing the water recovery. However, to avoid excessive trans-membrane pressures that could cause solution leakage, the flow rate of the pre-desalinated SW was no more than about twice the flow rate of the pre-concentrated solution. Higher flow rates in both compartments were used to reduce the relative detrimental effects of osmosis and/or electro-osmosis.

The typical duration of each test was between 90 and 120 minutes. Long-run tests were conducted for a duration up to height hours, showing a good stability of the plant. The accumulated operating time was of ~80 hours, with experiments performed intermittently (due to restrictions related to the COVID 19 pandemic) during a period of about one year. However, the performed experiments represent a meaningful set of tests, and the collected data provide interesting results and insights.

Errors in the measurements due to the parameters of the instruments (i.e., accuracy and resolution) were in the order of 0.1%. The error propagated in the calculation of the energy consumption remains in the same order of magnitude. Tests replicated under the same conditions showed a good reproducibility of the results (discrepancy in the order of 1%). For these reasons, error bars would be too small in the charts of the results, thus we did not report them.

Table 4. Set points adopted in the electromembrane pre-desalination stage(s). "N.A." means "not applicable" and indicates either quantities not fixed as set points but obtained as results (i.e., the voltage drop in stage 1 for the ED-ED-RO tests and the pre-desalinated SW outlet conductivity from stage 1 for the scRED-RED-RO tests) or non-pertinent quantities (i.e., parameters regarding stage 1 for the ED-RO tests). The feedwater temperature recorded in the tests is also reported.

Configuration	Test case	Pre-desalinated SW outlet flow rate [l/h]	Pre-concentrated solution (SW or TWW) outlet flow rate [l/h]	Pre-desalinated SW outlet conductivity from stage 1 [mS/cm]	Voltage drop in stage 1 [V]	Pre-desalinated SW outlet conductivity from stage 2 or single stage [mS/cm]	Feedwater temperature [°C]
ED-ED-RO	**1**	1,555	766	36	N.A.	26	24.1
	2	1,700	892	40	N.A.	26	22.4
	3	1,500	1,092	40	N.A.	26	21.9
	4	1,500	820	40	N.A.	25	21.9
	5	1,500	820	40	N.A.	30	19.4
	6	1,500	820	40	N.A.	26	15.8

	7	1,800	900	40	N.A.	26	15.3
ED-RO	**8**	1,555	766	N.A.	N.A.	32.6	26.8
scRED-ARED-RO	**9**	2,380	1,140	N.A.	0	33.4	27.2 (SW), 26.6 (TWW)
	10	2,380	1,140	N.A.	0	33	27.9 (SW), 26.6 (TWW)

289 *2.5 Figures of merit characterizing the pilot plant performance*

290 The feedwater ratio in the electromembrane pre-desalination process was defined as:

$$FR_{EM} = \frac{Q_{pre-des,in,EM}}{Q_{pre-d\ \ ,in,EM} + Q_{pre-conc,in,EM}} \quad (1)$$

291 where $Q_{pre-des,in,EM}$ and $Q_{pre-conc,in,EM}$ are the volume flow rates of the pre-desalted (seawater) and
292 pre-concentrated (seawater or TWW) solution, respectively, at the inlet of the EM stage. Water
293 recovery of the EM process, of the RO, and total water recovery were calculated as:

$$WR_{EM} = \frac{Q_{pre-des,out,EM}}{Q_{pre-des,in,EM} + Q_{pre-conc,in,EM}} \quad (2)$$

$$WR_{RO} = \frac{Q_{perm,RO}}{Q_{feed,RO}} \quad (3)$$

$$WR_{tot} = \frac{Q_{perm,RO}}{Q_{pre-des,in,EM} + Q_{pre-conc,in,EM}} \quad (4)$$

294 where $Q_{pre-d\ \ ,out,EM}$ is the volume flow rate of the pre-desalted seawater at the outlet of the EM
295 process, $Q_{perm,RO}$ and $Q_{feed,RO}$ are the volume flow rates of RO permeate and feed, respectively. The
296 pre-desalted seawater from the EM stage was collected in a tank and then pumped to the RO pressure
297 vessel. When the flow rate of pre-desalted seawater coincides with that of RO feed, the total water
298 recovery is simply given by $WR_{tot} = WR_{EM} \cdot WR_{RO}$.

299 The specific production of desalted water per membrane area, called "productivity", was calculated
300 for the EM processes and the RO as:

$$Prod_{EM} = \frac{Q_{pre-des,out,EM}}{A_{IEM}} \quad (5)$$

$$Prod_{RO} = \frac{Q_{perm,RO}}{A_{osm}} \quad (6)$$

where A_{IEM} and A_{osm} are the total areas of ion-exchange membranes in the EM stack(s) (either one or two) and in the RO modules. Clearly, the productivity of the RO process is the permeate flux.

The specific energy consumption of the EM process, of the RO, and the total specific energy consumption (excluding contributions of pre-treatment and auxiliary components) were calculated as:

$$SEC_{EM} = \frac{\sum_i \Delta V_i \cdot I_i}{Q_{pre-des,out,EM}} \quad (7)$$

$$SEC_{RO} = \frac{Q_{feed,RO} \cdot p_{feed,RO}/\eta_{pump,RO}}{Q_{perm,RO}} \quad (8)$$

$$SEC_{tot} = \frac{\sum_i \Delta V_i \cdot I_i + Q_{feed,RO} \cdot p_{feed,RO}/\eta_{pump,RO}}{Q_{perm,RO}} \quad (9)$$

where ΔV_i and I_i are the voltage drop and the electric current supplied to the *i*-th stack (i.e., stack 1 or 2, with zero values for one stack in the case of single-stage ED), $p_{feed,RO}$ is the pressure applied to the RO feed upstream the pressure vessel, and $\eta_{pump,RO}$ is the efficiency of the pump pressurizing the RO feed (assumed equal to 0.9 [58]). Note that the SEC of each desalination stage (either EM or RO) has been defined per unit volume of its product water. Therefore, $SEC_{tot} \neq SEC_{EM} + SEC_{RO}$. In Eqs. (7) and (9) the DC drive efficiency and the pumping power consumption of the EM stage(s) are omitted, as they were negligible. Indeed, the former quantity was higher than 95% [59], and the latter, evaluated from the measured values of pressure drop in the EM stage(s), was below 0.1 kWh/m^3.

The energy consumption of the pilot plant was also evaluated by considering the use of an energy recovery device (ERD). In this case, the *SEC* of the RO process can be estimated as:

$$SEC_{RO,ERD} = \frac{p_{feed,RO}}{\eta_{pump,RO}}\left[1 + \frac{1 - WR_{RO}}{WR_{RO}}(1 - \eta_{ERD})\right] \quad (10)$$

where η_{ERD} is the efficiency of the ERD (assumed equal to 0.9). Eq. (10) is obtained under the assumptions of equal flow rates sent through the ERD (pressure exchanger), negligible pressure drops in the pressure vessel, null pressure of the feed upstream the device and of the brine downstream the device, no mixing of the fluids, and equal efficiencies for the high- and low-pressure pumps. For the EM-RO integrated processes, the total energy consumption becomes:

$$SEC_{tot,ERD} = \frac{\sum_i \Delta V_i \cdot I_i}{Q_{perm,RO}} + \frac{p_{feed,RO}}{\eta_{pump,RO}}\left[1 + \frac{1 - WR_{RO}}{WR_{RO}}(1 - \eta_{ERD})\right] \quad (11)$$

2.6 Baseline case: standalone SWRO

A baseline case of standalone SWRO was considered as benchmark for the integrated pilot plant performance. The baseline case was simulated by the RO model presented in a previous work [38]. The 6-module RO system (Section 2.3) was simulated with the following fixed conditions: feed concentration of 38.57 g/L (Table 1), feed temperature equal to the average value of the experimental test cases (22.2 °C), permeate flow rate of 25 m^3/day, and water recovery equal to the average value of the WR_{tot} obtained with the integrated system (39.1%). The model predicted the pressure to be applied to the feed, the permeate concentration and the retentate concentration. The *SEC* was evaluated with Eqs. (8) and (10) for the case without the ERD and with the ERD, respectively.

In the previous work [38], the RO model had been validated with ROSA and WAVE modelling tools by DuPont, finding a very good agreement. Now the RO model has been validated against the experimental data collected with the pilot plant. As shown in Table 5, the model predicted the permeate flux with values of discrepancy with the experimental data of few percent. Larger

discrepancies were observed for the permeate conductivity. Overall, the agreement can be considered satisfactory, and the model can be considered reliable.

Table 5. Comparison between RO model predictions and experimental data from the pilot plant.

	Test case 1			**Test case 3**			**Test case 4**		
	Experimental	Model	Discrepancy	Experimental	Model	Discrepancy	Experimental	Model	Discrepancy
Permeate conductivity [µS/cm]	378.33	484.04	28%	309.46	368.08	19%	664.12	419.33	-37%
Permeate flux [L/(m^2 h)]	25.93	26.94	4%	30.78	31.22	1%	21.15	22.26	5%

Note that the complete model [38] for EM-RO integrated processes was validated with data from the pilot testing, but this is beyond the scope of the present study.

3 Results and Discussion

Results of the field-tests performed with the integrated pilot plant under different experimental conditions are summarized and discussed in the following. First, the electrical parameters of the electromembrane pre-desalination are presented. Then, the pressure applied in the RO stage and the permeate (product) conductivity are shown. Finally, the performance of the pilot plant is assessed by the main figures of merit.

3.1 Electromembrane pre-desalination: electrical parameters

The stack voltage and the current density applied in the EM pre-desalination to get the fixed setpoints (Table 4) are shown in Figure 5. In the two-stage ED experiments (test cases 1-7), the voltage drop was between ~46 and 110 V (Figure 5a). Note that the test cases 1-5 were characterized by high values of voltage drop in the first stage (~97-110 V), while it was significantly lower in the test cases 6-7 (~46-52 V). In the first tests, stack 1 exhibited some malfunctions that caused a high apparent

resistance. However, they were then resolved by a successful stack revamping (see Appendix). The voltage drop in the second stage of the ED experiments was lower than ~65 V, and stack 2 did not suffer from high resistance as much as stack 1 before the revamping operation.

In the single-stage ED experiment (test case 8), the voltage drop was ~45 V, which was close to the minimum value of ~37-38 V characterizing stack 2 (ARED stage) for the scRED-ARED experiments (test cases 9 and 10). Of course, these test cases had zero voltage in the scRED stage (stack 1).

The current density ranged between ~145 and 212 A/m^2 in all test cases, apart from the scRED stage of the scRED-ARED experiments (test cases 9 and 10), where it was just below 60 A/m^2, as shown in Figure 5b.

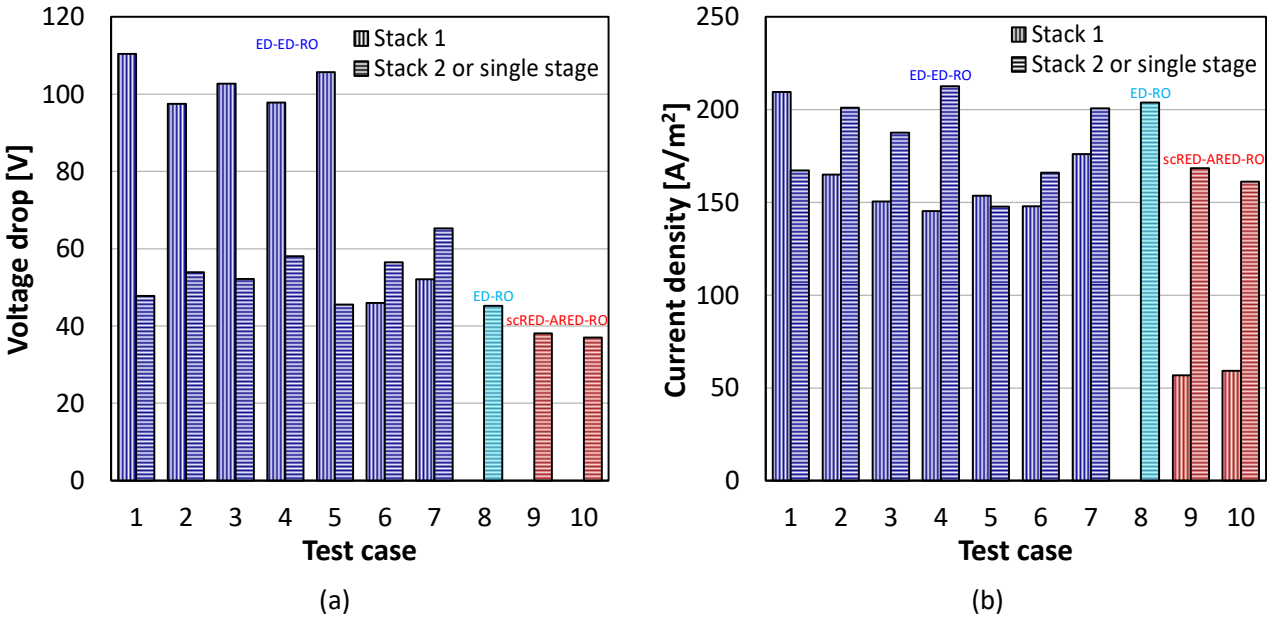

Figure 5. Voltage drop (a) and current density (b) in the electromembrane pre-desalination processes needed to yield the setpoints reported in Table 4. Note that the test case 8 is with single-stage ED before RO, and the test cases 9 and 10 are with scRED, hence with zero voltage drop, in the first stack. The test cases 6-10 were performed after stacks revamping.

From these results, it can be drawn that the power consumption in the EM pre-desalination (see Eq. (9)) was in the descending order ED-ED > ED > scRED-ARED. Even when the values of voltage and current of the different test cases were comparable, the ED-ED configuration involved a higher power due to the sum of two contributions, while the ED and scRED-ARED configurations had only one

stack consuming energy. Moreover, both voltage and current were higher in the single-stage ED configuration (test case 8) than in the scRED-ARED configuration (test cases 9 and 10). Moreover, the difference in the specific energy consumption between these two configurations will be accentuated by the higher flow rate of the pre-desalinated SW in the scRED-ARED cases (Table 4). Detailed data on the energy consumption will be reported and discussed in Section 3.3.

3.2 RO: applied pressure and product conductivity

Overall, the pressure applied to the RO feed (pre-desalinated seawater from the EM process) ranged from ~31 to 46 bar (Figure 6a). The permeate conductivity was lower than ~800 µS/cm in all the experiments, and equal to 540 µS/cm on average (Figure 6b), which means that drinking water quality for human use was achieved. The baseline case of the standalone SWRO required the highest pressure (~58 bar, Figure 6a) and yielded the highest permeate conductivity, equal to ~1068 µS/cm (Figure 6b). For an NaCl solution at 20 °C, this value of electrical conductivity corresponds to a concentration of 525 mg/L [60], which is closer to the TDS limit of 600 mg/L recommended by WHO guidelines [61].

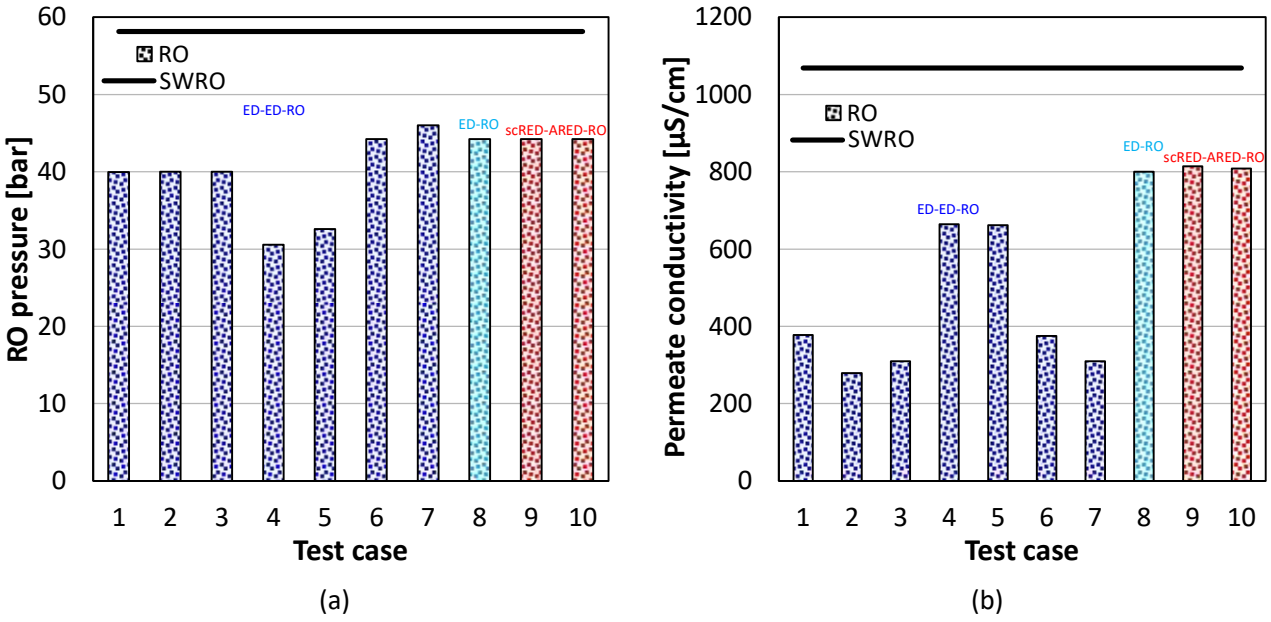

Figure 6. Pressure applied to the RO feed (a) and electrical conductivity of the RO permeate (b). The baseline case of the standalone SWRO is also reported.

385 The RO feed pressurization level also affected the water flux and thus the product flow rate, as will
386 be discussed in Section 3.3.

387 *3.3 Performance of the pilot plant*

388 Feedwater ratio and water recoveries are reported in Figure 7. On average, the feedwater ratio was
389 72%, which is larger than the water recovery of the EM stage, i.e., ~63% on average. This difference
390 can be explained by the occurrence of a net water transport resulting from osmosis and electro-
391 osmosis. In the ED tests, both mechanisms take place towards the same direction, i.e., from the pre-
392 desalinated solution to the pre-concentrated solution, causing a reduction of the flow rate of the pre-
393 desalinated seawater. In the test case 8, the halved IEM area reduced the difference between FR_{EM}
394 and WR_{EM}. In the scRED and ARED conditions, electro-osmosis is towards the opposite direction
395 with respect to osmosis. However, the values of WR_{EM} lower than those of FR_{EM} in the test cases 9
396 and 10 indicate that the electro-osmotic flux prevailed on the osmotic flux. The water recovery in the
397 RO stage was between 31% and 63%, with values higher than 50-60% in most test cases.

398 The total water recovery of the pilot plant with the hybrid EM-RO processes ranged from 27% to
399 51%. Note that WR_{tot} was not necessarily equal to the product of WR_{EM} times WR_{RO}, as the feed flow
400 rate in the RO stage was not always identical to the outlet flow rate from the pre-desalination stage.
401 It is worth noting that in the present scRED-ARED-RO configurations (test cases 9 and 10) the total
402 water recovery calculated with respect to seawater feed only (i.e., excluding the impaired water)
403 would be ~40%. Overall, the average water recovery of the hybrid pilot plant is 39.1%, corresponding
404 to the value imposed in the SWRO baseline case.

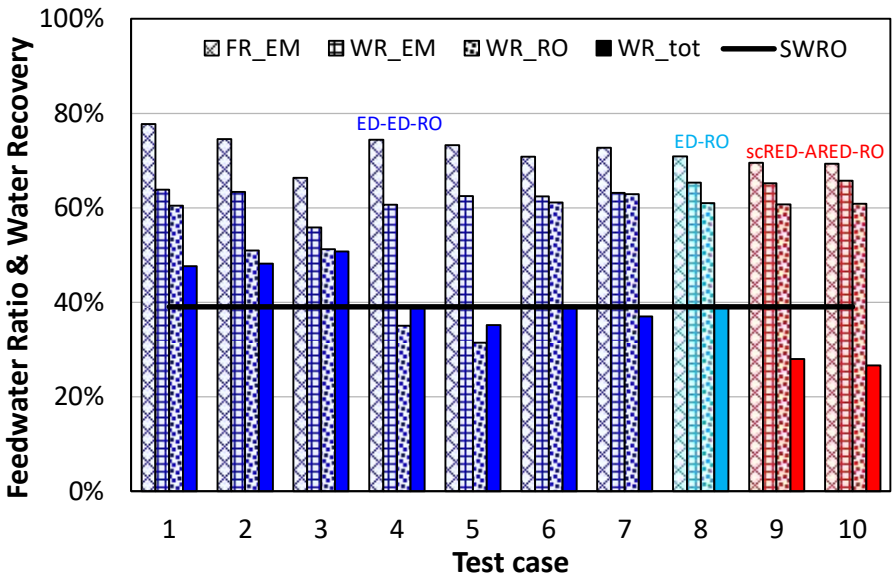

405

406 Figure 7. Feedwater ratio in the electromembrane pre-desalination (FR_{EM}) needed to yield the setpoints reported in Table
407 4, and water recovery achieved in the EM pre-desalination (WR_{EM}), in the RO stage (WR_{RO}) and in the combined EM-RO
408 process (WR_{tot}). The baseline case of the standalone SWRO is also reported.

409 The values of productivity achieved by the pilot plant are reported in Figure 8. In the two-stage ED
410 experiments, the productivity was ~7 L/(m^2 h), but this value was doubled in the single-stage ED (test
411 case 8). Higher flow rates of seawater were used in the scRED-ARED experiments (see Table 4), so
412 that the test cases 9 and 10 had a productivity of ~10 L/(m^2 h). The productivity of the RO stage
413 ranged from ~19 to 31 L/(m^2 h), with an average value of 23.4 L/(m^2 h), which was set for the
414 standalone SWRO baseline case. The obtained permeate flow rate, which can be simply calculated
415 by multiplying the RO productivity times the RO membrane area (44.6 m^2), was from 20.4 to 33.0
416 m^3/day.

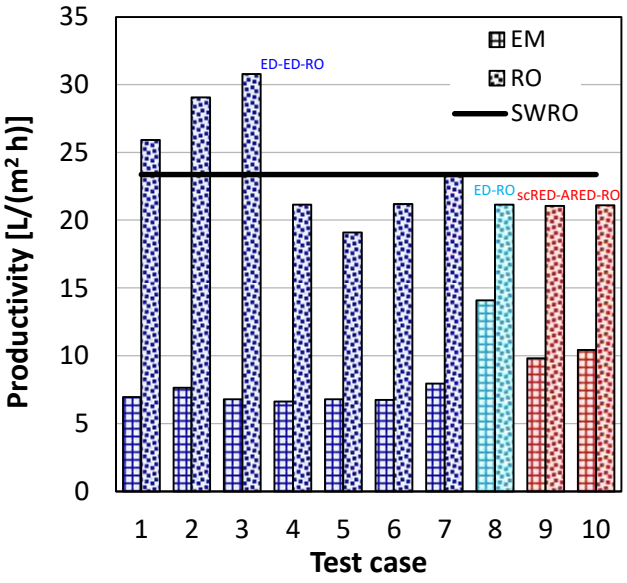

417

418 Figure 8. Productivity of the EM pre-desalination and of the RO stage. The baseline case of the standalone SWRO is also
419 reported.

420 The values of specific energy consumption of the pilot plant are reported in Figure 9 for two scenarios:
421 system without any ERD, and system provided with an ERD. Looking at the former case, the ED-
422 ED-RO configuration (test cases 1-7) had higher total energy consumptions (~5.6-8.4 kWh/m^3). It
423 was caused by a high energy-consuming EM pre-desalination, not only before stacks revamping (test
424 cases 1-5, with SEC_{EM} of ~2.9-3.9 kWh/m^3), but also after that (test cases 6 and 7, with SEC_{EM} of
425 ~2.1 and 2.4 kWh/m^3, respectively). The ED-RO configuration (test case 8), instead, showed an
426 energy consumption in the ED stage reduced to ~1.1 kWh/m^3 and simultaneously maintained a low
427 energy consumption, i.e., ~2.2 kWh/m^3, in the RO stage, yielding an SEC_{tot} of ~4.1 kWh/m^3. The
428 scRED-ARED-RO configuration (test cases 9 and 10) further reduced the values of SEC_{EM} (~0.54
429 kWh/m^3 on average), maintained the SEC_{RO} at ~2.3 kWh/m^3, and attained the minimum SEC_{tot} of
430 ~3.5 kWh/m^3. With respect to the test case 9, the test case 10 was conducted with a small reduction
431 in the setpoint of the conductivity of the pre-desalinated seawater (Table 4). However, due to some
432 variations in the feedwater conductivity (salinity and temperature) the test case 10 attained a slightly
433 lower SEC_{EM} and thus a lower SEC_{tot}. Under the operating conditions of the test cases 8, 9, and 10
434 without any ERD, the pilot plant exhibits values of SEC_{tot} (Eq. (9)) lower than the SEC of the

standalone SWRO baseline (SEC_{SWRO}, Eq. (8)), which was 4.6 kWh/m^3. Despite the additional contribution to the SEC_{tot} due to the EM processes, the EM-RO integrated system can be operated under conditions reducing the energy consumption compared to a standalone SWRO system.

In the scenario with the ERD, the energy consumption of the RO stage of the pilot plant ($SEC_{RO,ERD}$, Eq. (10)) and the total energy consumption ($SEC_{tot,ERD}$, Eq. (11)) were reduced on average by 42% and 18%, respectively, compared to the values obtained without the ERD (SEC_{RO} and SEC_{tot}, respectively). Instead, the energy consumption of the standalone SWRO configuration ($SEC_{SWRO,ERD}$, Eq. (10)) decreased by 55%, reaching 2.1 kWh/m^3, which is 23% smaller than the lowest $SEC_{tot,ERD}$ of the integrated system (test case 10). This occurs despite the SWRO system requires the highest pressure (Figure 6). Indeed, a comparison between Eq. (10) and Eq. (11) shows that the standalone SWRO configuration saves the energy consumption of the EM stage. Moreover, there is an effect of the water recovery. The SWRO baseline case was performed by imposing a water recovery equal to the average value of the total water recovery of the integrated system, which implies that it is higher than the average water recovery of the RO stage of the integrated system. Therefore, the higher pressure required by the SWRO configuration is counter-balanced by these effects, leading to a lower energy consumption.

However, the ED-RO (test case 8) and scRED-ARED-RO (test cases 9 and 10) configurations exhibit values of $SEC_{tot,ERD}$ comparable to the $SEC_{SWRO,ERD}$. The integrated system produced also a permeate with better quality (Figure 6). Another simulation of the standalone SWRO process was performed by fixing the permeate conductivity at the mean value obtained with the integrated system, showing that the feed pressure would exceed the maximum value indicated by the manufacturer of the RO module.

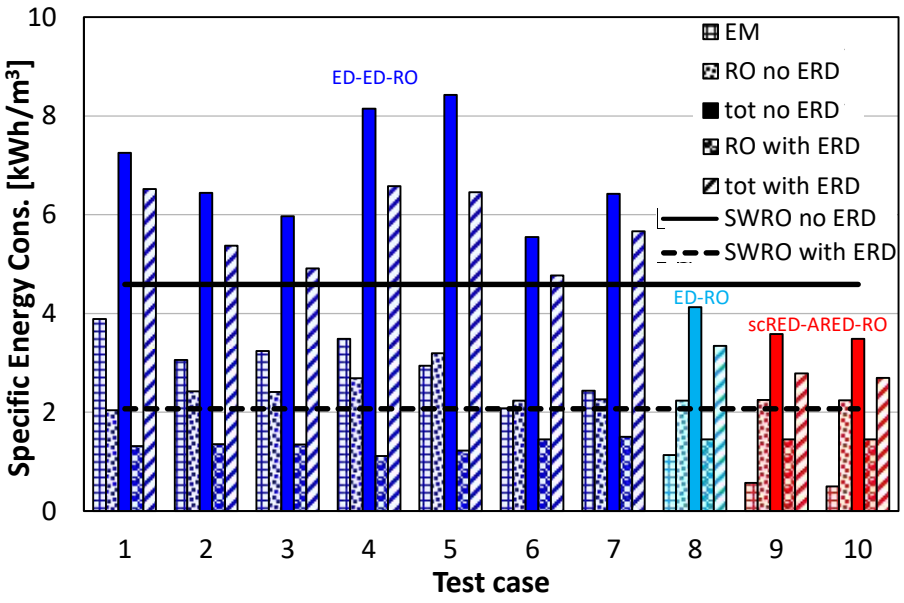

457

458 Figure 9. Specific energy consumption of the EM pre-desalination, of the RO stage, and of the combined process. Two
459 scenarios are considered for the RO (and thus for the total *SEC*): without ERD and with ERD. The baseline case of the
460 standalone SWRO is also reported.

461 ## 4 Conclusions

462 A hybrid desalination plant at pilot scale combining electromembrane (EM) processes with reverse
463 osmosis (RO) was demonstrated and tested for the first time for the production of drinking water from
464 real seawater. The nominal capacity of the plant was 25 m^3/day. Electrodialysis (ED), shortcut reverse
465 electrodialysis (scRED) and assisted reverse electrodialysis (ARED) were tested in the ED-ED-RO,
466 ED-RO, and scRED-ARED-RO configurations. In the scRED-ARED-RO test cases, treated
467 wastewater was used as impaired water acting as salt sink.

468 Pre-treatments, periodic polarity reversal, and chemical dosage were effective in the prevention of
469 fouling and scaling. However, cost-effective strategies should be assessed in future studies.

470 The total water recovery of the integrated plant was around 40%. The productivity of the EM
471 processes was ~7 L/(m^2 h) in the ED-ED test cases and ~10 L/(m^2 h) in the scRED-ARED test cases.
472 The maximum value of ~14 L/(m^2 h) was achieved by using a single stack (single-stage ED test). The
473 RO stage produced a permeate with a flux of ~20-30 L/(m^2 h). The lower productivity of the EM

474 treatment may represent an issue due to the high cost of ion-exchange membranes. The use of a lower
475 membrane area may be a possible strategy to reduce the capital cost.

476 The specific energy consumption was ~5.6-8.4 kWh/m^3 in the ED-ED-RO tests, while it reduced at
477 ~4.1 kWh/m^3 with the ED-RO configuration. Therefore, a lower area of ion-exchange membranes
478 can be beneficial for also reducing the operating cost. The scRED-ARED system further reduced the
479 energy consumption of the pre-desalination, reaching the minimum value of total energy consumption
480 of ~3.5 kWh/m^3. Therefore, the (A)RED process represents an interesting alternative for applications
481 with co-located seawater desalination plants and WWTPs.

482 Overall, the specific energy consumption of the integrated pilot plant was comparable with that of a
483 standalone SWRO system. In the absence of any ERD, ED-RO and scRED-ARED-RO tests with the
484 pilot plant outperformed the standalone SWRO system (4.6 kWh/m^3). By considering the use of an
485 efficient ERD, the energy consumption was lower for the SWRO (~20% smaller than the minimum
486 value of the integrated plant). However, the integrated system was able to produce drinking water
487 with better quality (average conductivity of 540 µS/cm, against ~1000 µS/cm of the SWRO system).

488 Customized modules should be developed to enhance the process performance. For example, RO
489 modules suitable for treating "diluted SW" may have a higher water permeability. Further studies
490 should address the techno-economic optimization of EM-RO integrated systems of industrial size by
491 considering both design and operating conditions. In this perspective, the availability of validated
492 modelling tools is crucial for the development of cost-effective systems to be proposed to the
493 desalination market.

494 **Acknowledgments**

495 This work was performed in the framework of the REvivED water project (Low energy solutions for
496 drinking water production by a REvival of ElectroDialysis systems). This project has received

497 funding from the European Union's Horizon 2020 Research and Innovation program under Grant
498 Agreement no. 685579 (www.revivedwater.eu).

499 The authors are grateful to Deukum GmbH for supplying the spacers, and to FACSA for providing
500 their facilities for the plant installation.

501 **Nomenclature**

502	A_{IEM}	total area of ion-exchange membranes used in the electromembrane process [m^2]
503	A_{osm}	total area of osmotic membrane used in the RO process [m^2]
504	FR_{EM}	feedwater ratio in the electromembrane process
505	I_i	electric current supplied to the *i*-th stack [A]
506	$Prod_{EM}$	productivity of the electromembrane process [L/(m^2 h)]
507	$Prod_{RO}$	productivity of the RO process [L/(m^2 h)]
508	$p_{feed,RO}$	pressure applied to the RO feed [Pa]
509	$Q_{feed,RO}$	flow rate of the RO feed [m^3/s]
510	$Q_{perm,RO}$	flow rate of the RO permeate [m^3/s]
511	$Q_{pre-conc,in,EM}$	flow rate of the pre-concentrated solution (seawater or treated wastewater) at the
512		inlet of the electromembrane process [m^3/s]
513	$Q_{pre-des,in,EM}$	flow rate of the pre-desalted seawater at the inlet of the electromembrane process
514		[m^3/s]
515	$Q_{pre-des,out,EM}$	flow rate of the pre-desalted seawater at the outlet of the electromembrane
516		process [m^3/s]
517	SEC_{EM}	specific energy consumption of the electromembrane process [kWh/m^3]

SEC_{RO}	specific energy consumption of the RO process [kWh/m^3]
$SEC_{RO,ERD}$	specific energy consumption of the RO process with the energy recovery device [kWh/m^3]
SEC_{SWRO}	specific energy consumption of the SWRO process [kWh/m^3]
$SEC_{SWRO,ERD}$	specific energy consumption of the SWRO process with the energy recovery device [kWh/m^3]
SEC_{tot}	total specific energy consumption of the integrated process [kWh/m^3]
$SEC_{tot,ERD}$	total specific energy consumption of the integrated process with the energy recovery device [kWh/m^3]
WR_{EM}	water recovery of the electromembrane process
WR_{RO}	water recovery of the RO process
WR_{tot}	total water recovery of the integrated process
Greek symbols	
ΔV_i	voltage drop at the *i*-th stack [V]
$\eta_{pump,RO}$	efficiency of the pump for the pressurization of the RO feed
η_{ERD}	efficiency of the energy recovery device

List of abbreviations

AEM	anion-exchange membrane
ARED	assisted reverse electrodialysis
CEM	cation-exchange membrane
ED	electrodialysis

EM	electromembrane
ERD	energy recovery device
ERS	electrode rinse solution
IEM	ion-exchange membrane
MF	Microfiltration
RED	reverse electrodialysis
RO	reverse osmosis
scRED	short-circuit reverse electrodialysis
SW	seawater
SWED	seawater electrodialysis
SWRO	seawater reverse osmosis
SEC	specific energy consumption
TDS	total dissolved solids
TWW	treated wastewater
UF	Ultrafiltration

5 Appendix: Overhaul and refurbishment of stacks

During the first testing period (test cases 1-5 in the main text), stack 1 exhibited a high electrical resistance (see Section 3.1). Therefore, both stacks were inspected to check their conditions from the inside. After removing the distribution side-plates, the first observation was a large amount of white deposition at the inlets/outlets of the channels close to the electrode chambers of stack 1 (Figure A1). The analysis of deposition samples detected both Ca and Mg salts, most likely $CaCO_3$ and $Mg(OH)_2$.

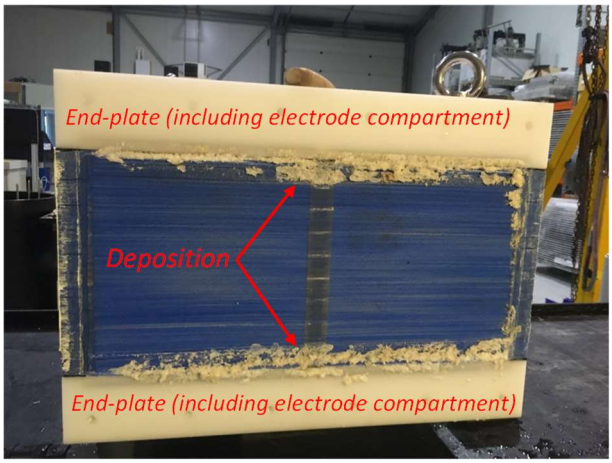

560

561 Figure A1. Stack 1 after taking away the distribution side-plates. The picture shows a white deposition at the outlet of the
562 channels near the electrode compartments (~5-10 cell pairs).

563 The stack overhaul detected (i) a severe damage (a hole) in the end-membranes, (ii) a loss of their
564 transport properties, and (iii) a severe internal leakage. Other membranes showed minor shift in
565 performance. It is not clear what caused the failure of stack 1, but probably it is related with a leakage
566 of ERS. It certainly occurred through the damaged end-membranes, but some initial leakage from the
567 gaskets (not perfect sealing) cannot be excluded. The triggered precipitation/deposition near the
568 electrode compartments caused a partial blockage of channels in those parts of the stack. This led to
569 a local over-depletion of ions in the desalting compartments and thus to a higher stack resistance. On
570 the other hand, it caused a lower limiting current density. Water splitting occurring at high voltage
571 favoured the precipitation of salts by a pH increase. This all might have caused the burned/damaged
572 membranes.

573 A stack revamping was then performed by replacing the damaged membranes. For stack 2, which did
574 not show problems, only the end-membranes were replaced. The new end-membranes (two layers)
575 used for both stacks were chlorine- and pH-resistant Fumatech membranes (Fumasep® F-10100), as
576 the ERS used in the tests after stack refurbishment was maintained at a pH of 3.5 and chlorine could
577 be formed due to NaCl diffusion. After revamping, the resistance of stack 1 was reduced by ~50%
578 and the tests did not show the issues that characterized the initial experiments.

579 Finally, it is worth mentioning that no fouling was observed on the membranes surface during the
580 stack overhaul, thus indicating that the pre-treatment was successful. In the experiments, the
581 conductivity of the concentrated seawater from the first stage was between ~68 and 82 mS/cm, while
582 that from the second stage was between ~85 and 97 mS/cm. However, no scaling was observed, likely
583 due to the acid dosage against carbonate precipitation and to the spacer effectiveness against
584 concentration polarization.

585 **References**

586 [1] E. Jones, M. Qadir, M.T.H. van Vliet, V. Smakhtin, S. Kang, The state of desalination and
587 brine production: A global outlook, Sci. Total Environ. 657 (2019) 1343–1356.
588 https://doi.org/10.1016/j.scitotenv.2018.12.076.

589 [2] J. Eke, A. Yusuf, A. Giwa, A. Sodiq, The global status of desalination: An assessment of
590 current desalination technologies, plants and capacity, Desalination. 495 (2020) 114633.
591 https://doi.org/10.1016/j.desal.2020.114633.

592 [3] L.F. Greenlee, D.F. Lawler, B.D. Freeman, B. Marrot, P. Moulin, Reverse osmosis
593 desalination: Water sources, technology, and today's challenges, Water Res. 43 (2009) 2317–
594 2348. https://doi.org/10.1016/j.watres.2009.03.010.

595 [4] M. Elimelech, W.A. Phillip, The future of seawater desalination: Energy, technology, and the
596 environment, Science (80-.). 333 (2011) 712–717. https://doi.org/10.1126/science.1200488.

597 [5] H. Nassrullah, S.F. Anis, R. Hashaikeh, N. Hilal, Energy for desalination: A state-of-the-art
598 review, Desalination. 491 (2020) 114569. https://doi.org/10.1016/j.desal.2020.114569.

599 [6] V.G. Gude, Desalination and sustainability – An appraisal and current perspective, Water Res.
600 89 (2016) 87–106. https://doi.org/10.1016/j.watres.2015.11.012.

601 [7] G. Amy, N. Ghaffour, Z. Li, L. Francis, R.V. Linares, T. Missimer, S. Lattemann, Membrane-
602 based seawater desalination: Present and future prospects, Desalination. 401 (2017) 16–21.
603 https://doi.org/10.1016/j.desal.2016.10.002.

604 [8] N. Voutchkov, Energy use for membrane seawater desalination – current status and trends,
605 Desalination. 431 (2018) 2–14. https://doi.org/10.1016/j.desal.2017.10.033.

606 [9] J. Kim, K. Park, D.R. Yang, S. Hong, A comprehensive review of energy consumption of
607 seawater reverse osmosis desalination plants, Appl. Energy. 254 (2019) 113652.
608 https://doi.org/10.1016/j.apenergy.2019.113652.

609 [10] C. Skuse, A. Gallego-Schmid, A. Azapagic, P. Gorgojo, Can emerging membrane-based
610 desalination technologies replace reverse osmosis?, Desalination. 500 (2021) 114844.
611 https://doi.org/10.1016/j.desal.2020.114844.

612 [11] A. Campione, L. Gurreri, M. Ciofalo, G. Micale, A. Tamburini, A. Cipollina, Electrodialysis
613 for water desalination: A critical assessment of recent developments on process fundamentals,
614 models and applications, Desalination. 434 (2018) 121–160.
615 https://doi.org/10.1016/j.desal.2017.12.044.

616 [12] F.E. Ahmed, A. Khalil, N. Hilal, Emerging desalination technologies: Current status,

challenges and future trends, Desalination. 517 (2021) 115183. https://doi.org/10.1016/j.desal.2021.115183.

[13] S.K. Patel, P.M. Biesheuvel, M. Elimelech, Energy Consumption of Brackish Water Desalination: Identifying the Sweet Spots for Electrodialysis and Reverse Osmosis, ACS ES&T Eng. (2021) acsestengg.0c00192. https://doi.org/10.1021/acsestengg.0c00192.

[14] A. Daniilidis, R. Herber, D.A. Vermaas, Upscale potential and financial feasibility of a reverse electrodialysis power plant, Appl. Energy. 119 (2014) 257–265. https://doi.org/10.1016/j.apenergy.2013.12.066.

[15] R.A. Tufa, S. Pawlowski, J. Veerman, K. Bouzek, E. Fontananova, G. di Profio, S. Velizarov, J. Goulão Crespo, K. Nijmeijer, E. Curcio, Progress and prospects in reverse electrodialysis for salinity gradient energy conversion and storage, Appl. Energy. 225 (2018) 290–331. https://doi.org/10.1016/j.apenergy.2018.04.111.

[16] R.W. Baker, Membrane Technology and Applications, John Wiley & Sons, Ltd, Chichester, UK, 2012. https://doi.org/10.1002/9781118359686.

[17] M.M. Generous, N.A.A. Qasem, U.A. Akbar, S.M. Zubair, Techno-economic assessment of electrodialysis and reverse osmosis desalination plants, Sep. Purif. Technol. 272 (2021) 118875. https://doi.org/10.1016/j.seppur.2021.118875.

[18] L. Bazinet, T.R. Geoffroy, Electrodialytic Processes: Market Overview, Membrane Phenomena, Recent Developments and Sustainable Strategies, Membranes (Basel). 10 (2020) 221. https://doi.org/10.3390/membranes10090221.

[19] L. Gurreri, A. Tamburini, A. Cipollina, G. Micale, Electrodialysis Applications in Wastewater Treatment for Environmental Protection and Resources Recovery: A Systematic Review on Progress and Perspectives, Membranes (Basel). 10 (2020) 146. https://doi.org/10.3390/membranes10070146.

[20] A. Campione, A. Cipollina, I.D.L. Bogle, L. Gurreri, A. Tamburini, M. Tedesco, G. Micale, A hierarchical model for novel schemes of electrodialysis desalination, Desalination. 465 (2019) 79–93. https://doi.org/10.1016/J.DESAL.2019.04.020.

[21] M. La Cerva, L. Gurreri, M. Tedesco, A. Cipollina, M. Ciofalo, A. Tamburini, G. Micale, Determination of limiting current density and current efficiency in electrodialysis units, Desalination. 445 (2018) 138–148. https://doi.org/10.1016/j.desal.2018.07.028.

[22] L. Gurreri, A. Filingeri, M. Ciofalo, A. Cipollina, M. Tedesco, A. Tamburini, G. Micale, Electrodialysis with asymmetrically profiled membranes: Influence of profiles geometry on desalination performance and limiting current phenomena, Desalination. 506 (2021) 115001. https://doi.org/10.1016/j.desal.2021.115001.

[23] G. Battaglia, L. Gurreri, M. Ciofalo, A. Cipollina, I.D.L. Bogle, A. Pirrotta, G. Micale, A 2-D model of electrodialysis stacks including the effects of membrane deformation, Desalination. 500 (2021) 114835. https://doi.org/10.1016/j.desal.2020.114835.

[24] G. Doornbusch, M. van der Wal, M. Tedesco, J. Post, K. Nijmeijer, Z. Borneman, Multistage electrodialysis for desalination of natural seawater, Desalination. 505 (2021) 114973. https://doi.org/10.1016/j.desal.2021.114973.

[25] G.J. Doornbusch, M. Tedesco, J.W. Post, Z. Borneman, K. Nijmeijer, Experimental investigation of multistage electrodialysis for seawater desalination, Desalination. 464 (2019) 105–114. https://doi.org/10.1016/J.DESAL.2019.04.025.

[26] G. Doornbusch, H. Swart, M. Tedesco, J. Post, Z. Borneman, K. Nijmeijer, Current utilization in electrodialysis: Electrode segmentation as alternative for multistaging, Desalination. 480

662 (2020) 114243. https://doi.org/10.1016/j.desal.2019.114243.

663 [27] G.J. Doornbusch, M. Bel, M. Tedesco, J.W. Post, Z. Borneman, K. Nijmeijer, Effect of
664 membrane area and membrane properties in multistage electrodialysis on seawater desalination
665 performance, J. Memb. Sci. 611 (2020) 118303.
666 https://doi.org/10.1016/j.memsci.2020.118303.

667 [28] J. Jang, Y. Kang, J.H. Han, K. Jang, C.M. Kim, I.S. Kim, Developments and future prospects
668 of reverse electrodialysis for salinity gradient power generation: Influence of ion exchange
669 membranes and electrodes, Desalination. 491 (2020) 114540.
670 https://doi.org/10.1016/j.desal.2020.114540.

671 [29] S. Pawlowski, R.M. Huertas, C.F. Galinha, J.G. Crespo, S. Velizarov, On operation of reverse
672 electrodialysis (RED) and membrane capacitive deionisation (MCDI) with natural saline
673 streams: A critical review, Desalination. 476 (2020) 114183.
674 https://doi.org/10.1016/J.DESAL.2019.114183.

675 [30] H. Tian, Y. Wang, Y. Pei, J.C. Crittenden, Unique applications and improvements of reverse
676 electrodialysis: A review and outlook, Appl. Energy. 262 (2020) 114482.
677 https://doi.org/10.1016/j.apenergy.2019.114482.

678 [31] A. Zoungrana, M. Çakmakci, From non-renewable energy to renewable by harvesting salinity
679 gradient power by reverse electrodialysis: A review, Int. J. Energy Res. 45 (2021) 3495–3522.
680 https://doi.org/10.1002/er.6062.

681 [32] A. Tamburini, A. Cipollina, M. Tedesco, L. Gurreri, M. Ciofalo, G. Micale, The REAPower
682 Project: Power Production From Saline Waters and Concentrated Brines, in: A. Basile, E.
683 Curcio, I. Inamuddin (Eds.), Curr. Trends Futur. Dev. Membr. - Membr. Desalin. Syst. Next
684 Gener., Elsevier, Amsterdam, 2019: pp. 407–448.
685 https://doi.org/https://doi.org/10.1016/B978-0-12-813551-8.00017-6.

686 [33] J.Y. Nam, K.S. Hwang, H.C. Kim, H. Jeong, H. Kim, E. Jwa, S.C. Yang, J. Choi, C.S. Kim,
687 J.H. Han, N. Jeong, Assessing the behavior of the feed-water constituents of a pilot-scale 1000-
688 cell-pair reverse electrodialysis with seawater and municipal wastewater effluent, Water Res.
689 148 (2019) 261–271. https://doi.org/10.1016/j.watres.2018.10.054.

690 [34] S. Mehdizadeh, Y. Kakihana, T. Abo, Q. Yuan, M. Higa, Power Generation Performance of a
691 Pilot-Scale Reverse Electrodialysis Using Monovalent Selective Ion-Exchange Membranes,
692 Membranes (Basel). 11 (2021) 27. https://doi.org/10.3390/membranes11010027.

693 [35] A.M. Hulme, C.J. Davey, S. Tyrrel, M. Pidou, E.J. McAdam, Scale-up of reverse
694 electrodialysis for energy generation from high concentration salinity gradients, J. Memb. Sci.
695 627 (2021) 119245. https://doi.org/10.1016/j.memsci.2021.119245.

696 [36] R. Pärnamäe, L. Gurreri, J. Post, W.J. van Egmond, A. Culcasi, M. Saakes, J. Cen, E. Goosen,
697 A. Tamburini, D.A. Vermaas, M. Tedesco, The Acid–Base Flow Battery: Sustainable Energy
698 Storage via Reversible Water Dissociation with Bipolar Membranes, Membranes (Basel). 10
699 (2020) 409. https://doi.org/10.3390/membranes10120409.

700 [37] A. Culcasi, L. Gurreri, G. Micale, A. Tamburini, Bipolar membrane reverse electrodialysis for
701 the sustainable recovery of energy from pH gradients of industrial wastewater: Performance
702 prediction by a validated process model, J. Environ. Manage. 287 (2021) 112319.
703 https://doi.org/10.1016/j.jenvman.2021.112319.

704 [38] M. La Cerva, L. Gurreri, A. Cipollina, A. Tamburini, M. Ciofalo, G. Micale, Modelling and
705 cost analysis of hybrid systems for seawater desalination: Electromembrane pre-treatments for
706 Reverse Osmosis, Desalination. 467 (2019) 175–195.
707 https://doi.org/10.1016/j.desal.2019.06.010.

[39] F.E. Ahmed, R. Hashaikeh, N. Hilal, Hybrid technologies: The future of energy efficient desalination – A review, Desalination. 495 (2020) 114659. https://doi.org/10.1016/j.desal.2020.114659.

[40] M. Herrero-Gonzalez, R. Ibañez, Chemical and Energy Recovery Alternatives in SWRO Desalination through Electro-Membrane Technologies, Appl. Sci. 11 (2021) 8100. https://doi.org/10.3390/app11178100.

[41] R.K. McGovern, S.M. Zubair, J.H. Lienhard V, The cost effectiveness of electrodialysis for diverse salinity applications, Desalination. 348 (2014) 57–65. https://doi.org/10.1016/j.desal.2014.06.010.

[42] R.K. McGovern, A.M. Weiner, L. Sun, C.G. Chambers, S.M. Zubair, J.H. Lienhard V, On the cost of electrodialysis for the desalination of high salinity feeds, Appl. Energy. 136 (2014) 649–661. https://doi.org/10.1016/j.apenergy.2014.09.050.

[43] A.H. Galama, M. Saakes, H. Bruning, H.H.M. Rijnaarts, J.W. Post, Seawater predesalination with electrodialysis, Desalination. 342 (2014) 61–69. https://doi.org/10.1016/j.desal.2013.07.012.

[44] J.W. Post, H. Huiting, E.R. Cornelissen, H.V.M. Hamelers, Pre-desalination with electro-membranes for SWRO, Desalin. Water Treat. 31 (2011) 296–304. https://doi.org/10.5004/dwt.2011.2400.

[45] T.N. Bitaw, K. Park, J. Kim, J.W. Chang, D.R. Yang, Low-recovery, -energy-consumption, -emission hybrid systems of seawater desalination: Energy optimization and cost analysis, Desalination. 468 (2019) 114085. https://doi.org/10.1016/j.desal.2019.114085.

[46] S. Thampy, G.R. Desale, V.K. Shahi, B.S. Makwana, P.K. Ghosh, Development of hybrid electrodialysis-reverse osmosis domestic desalination unit for high recovery of product water, Desalination. 282 (2011) 104–108. https://doi.org/10.1016/j.desal.2011.08.060.

[47] J.M. Wreyford, J.E. Dykstra, K. Wetser, H. Bruning, H.H.M. Rijnaarts, Modelling framework for desalination treatment train comparison applied to brackish water sources, Desalination. 494 (2020) 114632. https://doi.org/10.1016/j.desal.2020.114632.

[48] B.M. Yang, J.M. Li, Z.Y. You, W.L. Lai, C.M. Kao, Using integrated electrodialysis and RO hybrid system to remediate and reclaim perchlorate-contaminated groundwater, Desalination. 480 (2020) 114377. https://doi.org/10.1016/j.desal.2020.114377.

[49] K. Loganathan, P. Chelme-Ayala, M. Gamal El-Din, Treatment of basal water using a hybrid electrodialysis reversal-reverse osmosis system combined with a low-temperature crystallizer for near-zero liquid discharge, Desalination. 363 (2015) 92–98. https://doi.org/10.1016/j.desal.2015.01.020.

[50] X. Zhang, C. Zhang, F. Meng, C. Wang, P. Ren, Q. Zou, J. Luan, Near-zero liquid discharge of desulfurization wastewater by electrodialysis-reverse osmosis hybrid system, J. Water Process Eng. 40 (2021) 101962. https://doi.org/10.1016/j.jwpe.2021.101962.

[51] Y. Mei, C.Y. Tang, Co-locating reverse electrodialysis with reverse osmosis desalination: Synergies and implications, J. Memb. Sci. 539 (2017) 305–312. https://doi.org/10.1016/j.memsci.2017.06.014.

[52] L. Gurreri, G. Battaglia, A. Tamburini, A. Cipollina, G. Micale, M. Ciofalo, Multi-physical modelling of reverse electrodialysis, Desalination. 423 (2017) 52–64. https://doi.org/10.1016/j.desal.2017.09.006.

[53] M. Ciofalo, M. La Cerva, M. Di Liberto, L. Gurreri, A. Cipollina, G. Micale, Optimization of net power density in Reverse Electrodialysis, Energy. 181 (2019) 576–588.

https://doi.org/10.1016/j.energy.2019.05.183.

[54] L. Gómez-Coma, V.M. Ortiz-Martínez, M. Fallanza, A. Ortiz, R. Ibañez, I. Ortiz, Blue energy for sustainable water reclamation in WWTPs, J. Water Process Eng. 33 (2020) 101020. https://doi.org/10.1016/j.jwpe.2019.101020.

[55] W. Li, W.B. Krantz, E.R. Cornelissen, J.W. Post, A.R.D. Verliefde, C.Y. Tang, A novel hybrid process of reverse electrodialysis and reverse osmosis for low energy seawater desalination and brine management, Appl. Energy. 104 (2013) 592–602. https://doi.org/10.1016/j.apenergy.2012.11.064.

[56] M. Vanoppen, E. Criel, S. Andersen, A.R.D. Verliefde, Assisted Reverse Electrodialysis : a Novel Technique To decrease reverse osmosis energy demand, AWWA / AMTA Membr. Technol. Conf. Pap. 32 (2016) 1–12. https://biblio.ugent.be/publication/7098263 (accessed October 18, 2018).

[57] M. Vanoppen, E. Criel, G. Walpot, D.A. Vermaas, A. Verliefde, Assisted reverse electrodialysis—principles, mechanisms, and potential, Npj Clean Water. 1 (2018) 9. https://doi.org/10.1038/s41545-018-0010-1.

[58] Danfoss, The heart of seawater RO systems: Rugged APP high-pressure pumps, https://assets.danfoss.com/documents/187154/AD243586503052en-001102.pdf (accessed November 25, 2021).

[59] SM15K series Products, Delta-Elektronika.nl, https://www.delta-elektronika.nl/en/products/bidirectional-dc-power-supplies-15kw-sm15k-series.html (accessed November 25, 2021).

[60] S.S. Islam, R.L. Gupta, K. Ismail, Extension of the Falkenhagen-Leist–Kelbg Equation to the Electrical Conductance of Concentrated Aqueous Electrolytes, J. Chem. Eng. Data. 36 (1991) 102–104. https://doi.org/10.1021/je00001a031.

[61] WHO, Guidelines for Drinking-water Quality, 2017.